Mie correction of spectra from silica beads embedded in resin matrix

J. Solheim[1], S. Sirovica[2], O. Addison[3,4] and A. Kohler[1]

[1] Faculty of Science and Technology, Norwegian University of Life Sciences, Ås, Norway; [2] Aston Institute of Materials Research and Aston Research Centre for Healthy Ageing, University of Aston, Birmingham, B4 7ET, UK; [3] Biomaterials Unit, School of Dentistry, University of Birmingham, Birmingham, B4 6NN, UK; [4] Faculty of Medicine and Dentistry, University of Alberta, Edmonton, Canada.

Keywords: Mie scattering, infrared images, preprocessing

Abstract

Strong scatter effects appear in infrared microscopy when the morphology is changing on a scale comparable to the wavelength of the incident radiation. They have been interpreted as Mie scattering [1], and are particularly strong when the shape of the sample is approximately spherical. Mie scattering introduces broad oscillatory structures in the baseline, as well as peak shifts due to dispersion in the refractive index of the sample. When these features are present in the absorbance spectra, the spectral analysis is severely hampered and it is therefore desirable to remove the Mie scattering signatures from the spectra.

Since the Mie correction based on Extended Multiplicative Signal Correction (EMSC) was introduced in 2008 [2], various methods have been proposed for removing Mie scattering from infrared absorbance spectra [3-5]. The current state of the art Mie correction algorithm, the Mie extinction EMSC (ME-EMSC), has proven to successfully model and remove Mie scattering from infrared spectra of biological samples. While we incorporated a consistent, complete and more complex model of the Mie extinction, we decreased the computational costs compared to the previous Mie correction algorithms.

In this study, we apply the ME-EMSC code to infrared hyperspectral imaging data of non-biological samples. We demonstrate that strong scatter distortions in hyperspectral images of silica beads embedded in a resin matrix can be corrected by the ME-EMSC algorithm. Further, we considered practical issues for the treatment of infrared images containing large amounts of spectra, such as filtering of input spectra for the ME-EMSC optimization and a quality test of output spectra. In the present study, we suggest strategies for quality controlling input and output spectra for the ME-EMSC algorithm.

1. Scattering of light by spherical objects

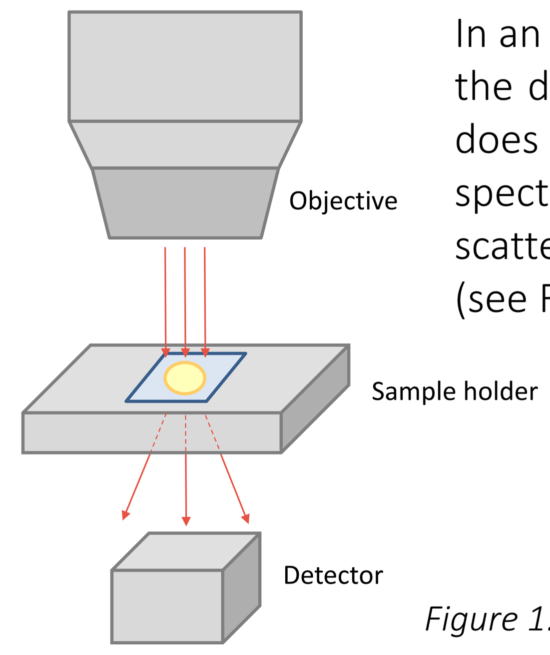

In an ideal infrared transmission measurement, radiation is either absorbed by the sample or it reaches the detector. However, when the incoming radiation is scattered by the sample, part of the radiation does not reach detector because of scattering resulting in scattering features in the absorbance spectra (Fig. 1). If the sample is spherical, the scattering takes on a particular form called Mie scattering. Mie scattering leads to gross oscillatory structures in the baseline of the absorbance spectra (see Fig. 2). Analytical solutions to scattering off a sphere were developed by Mie in 1908 [7]. In the Mie Extinction EMSC model, the van de Hulst approximation is employed for estimating and separating the scattering and chemical features in the absorbance spectra [8]. For calculating the scattering, the radius and the refractive index is needed. Since these parameters often remain unknown, the algorithm is initialized by providing relevant parameter ranges (see Fig. 3).

Figure 1: scattering in an infrared transmission experiment

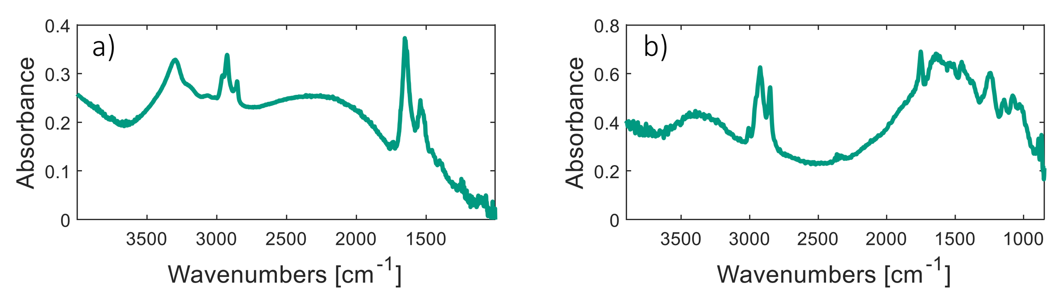

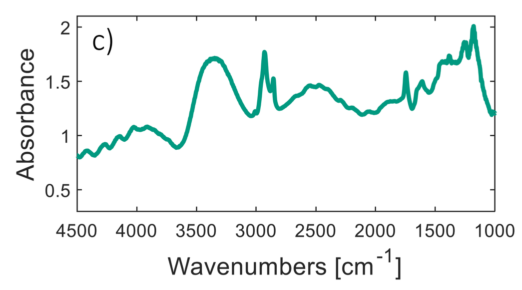

Figure 2: the apparent absorbance spectra which shows Mie scattering features for (a) a lung cancer cell [2] (b) a lipid body in a filamentous fungi and (c) a pollen grain from Juniperus Excelsa.

2. The ME-EMSC algorithm

The Mie Extinction EMSC is a special form of the model-based preprocessing technique EMSC. The scattering is estimated by calculating multiple realizations with rigorous Mie theory, based on a predefined parameter space. The multiple solutions are compressed by PCA and included in the ME-EMSC as the loadings, p_i (see step 4 and 5 in Fig. 3). One of the parameters needed for calculating the scattering is the imaginary part of the refractive index of the sample. This parameter is proportional to the pure absorbance of the sample, i.e. the spectrum we aim to retrieve. Therefore, the algorithm is initialized by providing a reference spectrum which is close to the pure absorbance spectrum. In each iteration, the chemical differences between the pure absorbance and the reference are gradually recovered, leading to the model becoming more precise. When the model converges, and the residuals stabilize, the iterative process is terminated.

Initialization

$Z_{app}(\tilde{\nu}) \sim$ measured spectrum
$Z_{ref}(\tilde{\nu}) \sim$ reference

Parameters:
$a \in [a_1, a_2] \sim$ radius
$n \in [n_1, n_2] \sim$ constant part of real part of refractive index
$h \sim$ scaling parameter

Step 1 - Estimate the imaginary part of the refractive index

$n' \sim Z_{ref}$

Step 2 - Estimate the fluctuating part of the real part of the refractive index via the Kramers-Kronig relation

$n' \rightarrow n_{kk}$

Step 3 - Calculate extinction efficiency Q_{ext}

$$Q_{ext}(\tilde{\nu}) \approx 2 - 4e^{-\rho \tan\beta} \frac{\cos\beta}{\rho} \sin(\rho - \beta) - 4e^{-\rho \tan\beta} \left(\frac{\cos\beta}{\rho}\right)^2 \cos(\rho - 2\beta) + 4\left(\frac{\cos\beta}{\rho}\right)^2 \cos 2\beta$$

The curves are made orthogonal to Z_{ref}

Step 4 - Decomposition via PCA

$Q_{ext} = TP' + E$

Step 5 - Mie Extinction EMSC

$$Z_{app}(\tilde{\nu}) = c + bZ_{ref}(\tilde{\nu}) + \sum_{i=1}^{A_{opt}} g_i p_i(\tilde{\nu}) + \epsilon(\tilde{\nu})$$

Step 6 - Estimate $Z_{corrected}$

$$Z_{corrected}(\tilde{\nu}) = \frac{(Z_{app}(\tilde{\nu}) - c - \sum_{i=1}^{A_{opt}} g_i p_i(\tilde{\nu}))}{b}$$

Stop-criterion
Terminates when RMSE is stabilized

Step 7 - Set corrected spectrum as reference

$Z_{ref}(\tilde{\nu}) = Z_{corrected}(\tilde{\nu})$

Output

$Z_{corrected}(\tilde{\nu})$

Figure 3: the iterative Mie Extinction EMSC algorithm. By estimating and removing the scattering, the pure absorbance spectrum is gradually retrieved. A better estimation of the pure absorbance spectrum leads to a more precise model.

3. Correcting spectra from silica beads in a resin matrix

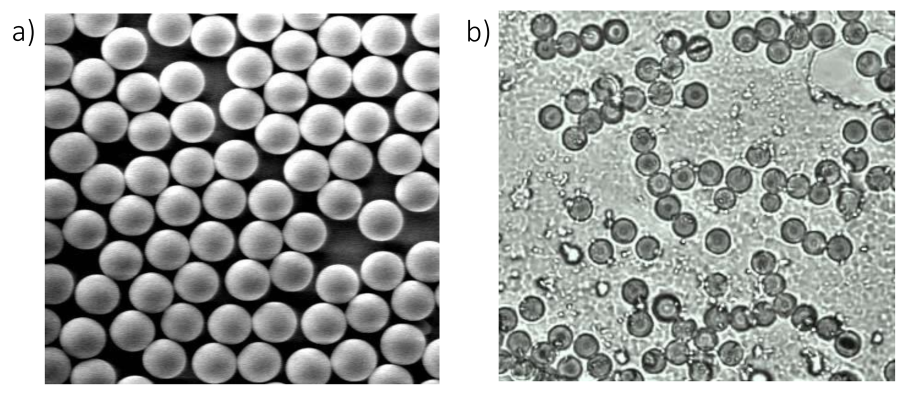

Figure 4: (a) scanning electron microscopy image of the silica beads (by courtesy of Cospheric [8]), (b) visual microscopic image of silica beads embedded in resin.

Hyperspectral images of silica beads embedded in a resin matrix (Fig. 4) were collected with a multi-beam synchrotron source coupled with an IR microscope at the IRENI beamline at the Synchrotron Radiation Center. Due to the spherical silica beads, the infrared spectra were distorted by Mie scattering. The Mie scattering was successfully estimated and removed from the spectra, such that the pure absorbance spectra were retrieved (see Fig. 5).

The quality test workflow presented below in Fig. 6 was used to filter the input and output spectra for the algorithm.

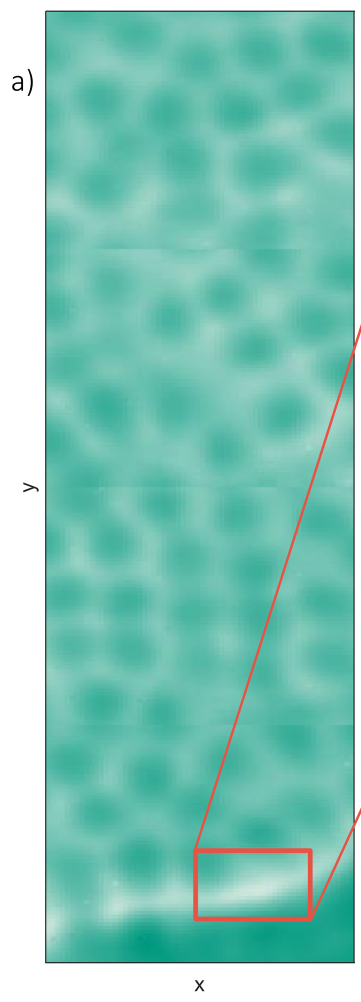

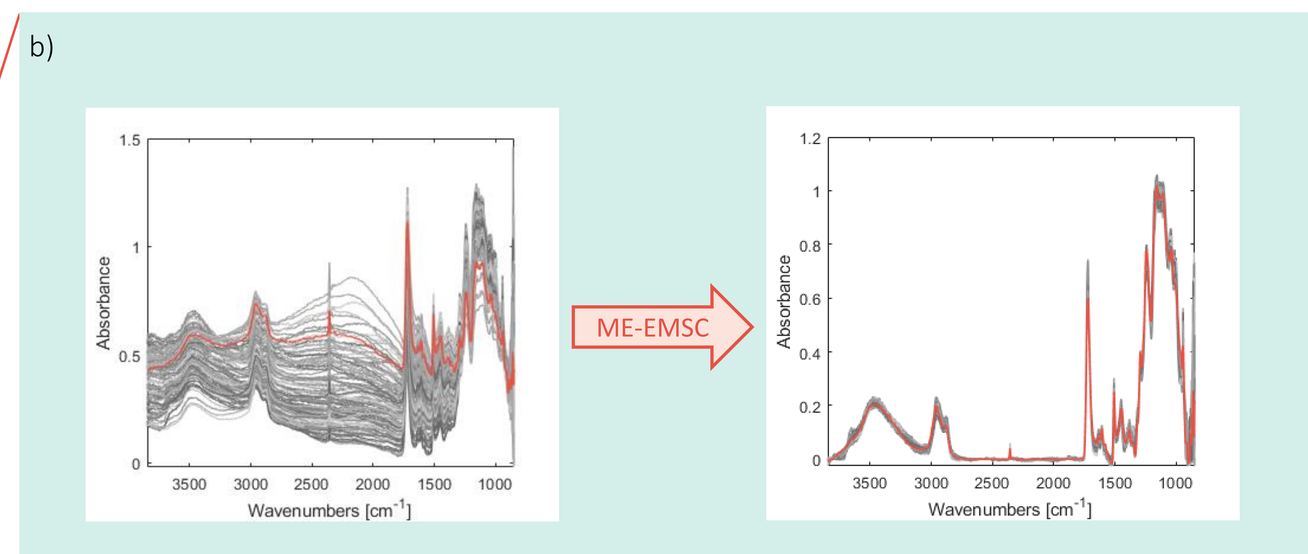

Figure 5: (a) Plot of a hyperspectral image of silica beads embedded in a resin matrix at 1720 cm-1, and (b) a selection of raw spectra and their respective corrected spectra.

4. Quality control workflow

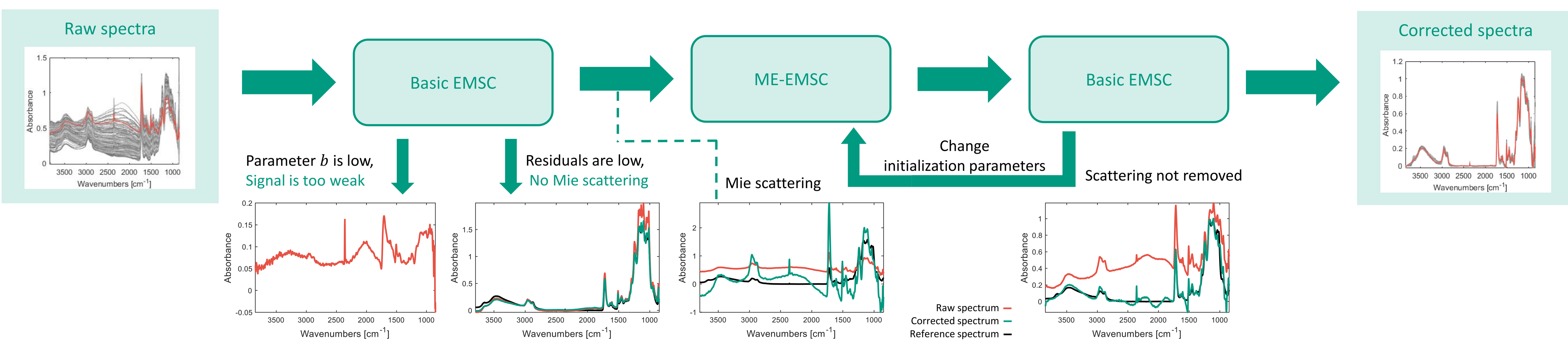

Figure 6: By employing a basic EMSC model prior to the ME-EMSC, we are able to filter out background spectra and spectra with no Mie scattering features. A basic EMSC can also be employed subsequent to the ME-EMSC model as a quality control of the corrected spectra. If the scattering features are not completely removed, we send the spectrum back to the ME-EMSC with adjusted initialization parameters.

Conclusions

- Spectra of non-biological samples which are affected by Mie scattering can be corrected by the ME-EMSC algorithm.
- A basic EMSC model can be employed to filter out spectra with low signal or no Mie scattering signatures prior to the ME-EMSC correction.
- A quality control of the corrected spectra can be performed with a basic EMSC model subsequent to the ME-EMSC correction.

Acknowledgements

The authors would like to acknowledge C. J. Hirschmugl, E. C. Mattson and E. Aboualizadeh from the IRENI beamline (the Synchrotron Radiation Center), R. A. Martin at Aston University, F. Borondics and C. Sandt at the SMIS beamline (Synchrotron SOLEIL), and S. Dzurendová, B. Zimmermann and V. Shapaval at the Norwegian University of Life Sciences for providing experimental data.

[1] Mohlenhoff, B., Romeo, M., Diem, M., & Wood, B. R. (2005). Biophysical journal, 88(5), 3635-3640.
[2] Kohler, A., Sule-Suso, J., Sockalingum, G. D., Tobin, M., Bahrami, F., Yang, Y., ... & Martens, H. (2008). Appl. Spectrosc., 62(3), 259-266.
[3] Bassan, P., Kohler, A., Martens, H., Lee, J., Byrne, H. J., Dumas, P., ... & Gardner, P. (2010). Analyst, 135(2), 268-277.
[4] van Dijk, T., Mayerich, D., Carney, P. S., & Bhargava, R. (2013). Appl. Spectrosc., 67(5), 546-552.
[5] Konevskikh, T., Lukacs, R., Blümel, R., Ponossov, A., & Kohler, A. (2016). Mie scatter corrections in single cell infrared microspectroscopy. Faraday discussions, 187, 235-257.
[6] Solheim, J., Gunko, E., Petersen, D., Großerüschkamp, F., Gerwert, K., & Kohler, A. (2019). J. Biophotonics, e201800415.
[7] Mie, G. (1908). Beiträge zur Optik trüber Medien, speziell kolloidaler Metallösungen. Annalen der physik, 330(3), 377-445.
[8] Hulst, H. C., & van de Hulst, H. C. (1981). Light scattering by small particles. Courier Corporation.
[9] Cospheric Nano 2019, *Nanoparticles*, viewed 13.08.2019, <https://www.nanospheres.com/>.

Norwegian University of Life Sciences

www.nmbu.no

BioSpec Norway